Development 137, 953-961 (2010) doi:10.1242/dev.041939

A conditional mutation in *Arabidopsis thaliana* separase induces chromosome non-disjunction, aberrant morphogenesis and cyclin B1;1 stability

Shuang Wu[1], Wolf-Rüdiger Scheible[2], Dana Schindelasch[2], Hilde Van Den Daele[3,4], Lieven De Veylder[3,4] and Tobias I. Baskin[1,*]

SUMMARY

The caspase family protease, separase, is required at anaphase onset to cleave the cohesin complex, which joins sister chromatids. However, among eukaryotes, separases have acquired novel functions. Here, we show that *Arabidopsis thaliana radially swollen 4* (*rsw4*), a temperature-sensitive mutant isolated previously on the basis of root swelling, harbors a mutation in *At4g22970*, the *A. thaliana* separase. Loss of separase function in *rsw4* at the restrictive temperature is indicated by the widespread failure of replicated chromosomes to disjoin. Surprisingly, *rsw4* has neither pronounced cell cycle arrest nor anomalous spindle formation, which occur in other eukaryotes upon loss of separase activity. However, *rsw4* roots have disorganized cortical microtubules and accumulate the mitosis-specific cyclin, cyclin B1;1, excessive levels of which have been associated with altered microtubules and morphology. Cyclin B1;1 also accumulates in certain backgrounds in response to DNA damage, but we find no evidence for aberrant responses to DNA damage in *rsw4*. Our characterization of *rsw4* leads us to hypothesize that plant separase, in addition to cleaving cohesin, regulates cyclin B1;1, with profound ramifications for morphogenesis.

KEY WORDS: *Arabidopsis thaliana*, DNA damage, Microtubules, Mitosis, *radially swollen 4*, Root morphology

INTRODUCTION

Plants build organs throughout their lives. Continual organogenesis endows the plant with plasticity in terms of ultimate size and fecundity, and allows the plant to acclimate to an altered environment by producing new organs with appropriate modifications. Plants develop, post-embryonically, from groups of pluripotent cells called meristems. A meristem generates cells that will acquire mature functions while simultaneously maintaining a population of proliferating cells. Conceptually, meristems allow the plant to keep making organs in much the same way as stem cells allow an animal organ to replace its cells.

Understanding the control of cell division is thus essential to an understanding of plant development. Generally, among eukaryotes, major features of the cell cycle and its regulation are strikingly conserved. However, when comparing a given protein among taxa, one often finds differences, sometimes fundamental ones.

The work reported here concerns the protein separase, which is a protease that is activated at the onset of anaphase to cleave the cohesin complex, which holds sister chromatids together (Onn et al., 2008). Separase targets the α-kleisin subunit of the cohesin complex. When separase activity is absent, chromosomes invariably fail to disjoin, causing chromosome breakage and multinucleate cells. Non-disjunction following separase inhibition has been reported in fungi [fission and budding yeasts and *Aspergillus nidulans* (Nasmyth et al., 2000)], *Caenorhabditis elegans* at both mitosis and meiosis (Siomos et al., 2001), *Drosophila melanogaster* (Jäger et al., 2001), various vertebrates (Papi et al., 2005; Kumada et al., 2006; Wirth et al., 2006; Shepard et al., 2007) and plant meiocytes (Liu and Makaroff, 2006). These results support the notion that separase activation at the onset of anaphase to disjoin chromatids is a widely conserved, if not ubiquitous, feature of the eukaryotic cell cycle.

Not surprisingly for a process as fundamental as the separation of chromosomes, separase is subject to a web of regulatory interactions. Some of these regulatory controls differ among organisms. Also, separase itself has been reported to have activities in addition to cleaving cohesin (Queralt and Uhlmann, 2005). For example, in budding yeast, separase plays a role in stabilizing microtubule dynamics of the anaphase spindle and in driving exit from M phase (Higuchi and Uhlmann, 2005; Baskerville et al., 2008). In *C. elegans*, separase is required for the secretion of the embryonic eggshell (Bembenek et al., 2007), and in *D. melanogaster* embryos separase deficiency has been associated with pseudostratification of the epithelium (Pandey et al., 2005). Finally, in human tissue culture cells, separase has been reported to be required for proper entry into M phase and spindle assembly (Giménez-Abián et al., 2005; Papi et al., 2005; Sak et al., 2008). Therefore, although all eukaryotic species examined use separase to cleave cohesin at anaphase onset, species appear to differ in how separase activity is regulated and to what extent the protein has acquired other functions.

Separase is an essential gene; therefore, studies of separase loss-of-function have, for the most part, been limited to tissue culture or early embryos. We know little about how separase acts in the cells of a mature organism or during development. This can be productively explored in plants because of their substantial, on-

[1]Biology Department, University of Massachusetts Amherst, 611 N. Pleasant St, Amherst, MA 01003, USA. [2]Max-Planck Institute for Molecular Plant Physiology, Science Park Golm, Am Mühlenberg 1, 14476 Potsdam, Germany. [3]Department of Plant Systems Biology, Flanders Institute for Biotechnology (VIB), 9052 Gent, Belgium. [4]Department of Plant Biotechnology and Genetics, Ghent University, 9052 Gent, Belgium.

*Author for correspondence (baskin@bio.umass.edu)

Accepted 15 January 2010

going cell division. The root is particularly useful because it is accessible to observation, is organized linearly and grows indeterminately.

Here, we report that *radially swollen 4* (*rsw4*), a temperature-sensitive mutant of *A. thaliana* isolated on the basis of aberrant root morphology (Wiedemeier et al., 2002), contains a mutation in the single-copy gene for separase. Consistently, *rsw4* plants have defective disjunction in mitotic root cells; unexpectedly, they also have defective cortical microtubule organization and accumulate cyclin B1;1.

MATERIALS AND METHODS

Plant material and growth

Plant material was *Arabidopsis thaliana* L. (Heynh), Columbia background. Plant growth was as described (Bannigan et al., 2006). The *rsw4* line was described previously (Wiedemeier et al., 2002). The GFP-tubulin reporter line expresses GFP fused to the *A. thaliana* β-tubulin 6 (*TUB6*) gene (Bannigan et al., 2006). The GFP-histone lines express GFP fused to the *A. thaliana* histone H3.3 gene (*At5g10980*) and were made by Keith Earley and Craig Pikaard (Washington University of St Louis). For each reporter, two transgenic lines, representing independent transformants with the same construct, were crossed onto *rsw4* and, from the F2, plants that were homozygous for *rsw4* and brightly fluorescent were selected by visual inspection and bulked up. Cell production rates, and the spatial profile of elemental elongation rate, were measured as described (Rahman et al., 2007).

Molecular identification of *RSW4*

For mapping, DNA samples of 1152 plants from an F2 population created from crossing *rsw4* and Landsberg *erecta*, and a set of 12 SSLP and CAPS markers (see Table S1 in the supplementary material) designed from information provided by The Arabidopsis Information Resource (http://www.arabidopsis.org), were used to map *RSW4* between markers mpi120 and mpi130 (see Table S1 in the supplementary material) in a ~56 kb region of chromosome 4, according to the procedures described (Lukowitz et al., 2000).

For complementation, colony hybridization (following the manufacturer's manual; Roche, Indianapolis, IN, USA) with five sequence-specific digoxigenin-11-dUTP-labeled DNA probes (336 to 542 bp; see Fig. 1B, asterisks) was used to isolate 32 clones covering the 56 kb *RSW4*-containing interval from a genomic cosmid library constructed in the binary vector pBIC20 (Meyer et al., 1994). A set of seven clones covering the interval was identified by multiplex PCR using the same primer pairs that amplified the hybridization probes. Mutant *rsw4* plants were transformed by *Agrobacterium tumefaciens* (GV3101) carrying cosmid clones according to Clough and Bent (Clough and Bent, 1998), and T1 transformants were selected on half-strength Murashige and Skoog plates containing kanamycin (50 μg/ml). Surface-sterilized T2 progeny of the transgenic T1 plants were grown on vertical agar plates supplemented with 1% sucrose for 7 days (5 days at 22°C followed by 2 days at 30°C) and scored for swollen root tips.

For sequencing, genomic DNA was prepared using a cetyl-trimethylammonium bromide-detergent extraction method (Lukowitz et al., 2000). Four DNA fragments (2209, 2491, 2814 and 3155 bp) encompassing the entire *RSW4* (*At4g22970*) coding sequence were amplified independently by PCR, three times from wild type and *rsw4* using specific primer pairs and a mixture of Taq and proofreading Pfu polymerases (Promega, Madison, WI, USA). Cycle sequencing of both strands of the PCR products was performed with a set of thirty primers and Big-Dye dideoxy terminator reaction mix (Applied Biosystems, Foster City, CA, USA), and products were resolved on an ABI310 sequencer. Likewise, a 1936 bp genomic fragment containing *At4g22980* was amplified by PCR and sequenced with a set of six primers.

Real-time quantitative PCR

Protocols for real-time quantitative PCR were as described previously (Czechowski et al., 2004; Czechowski et al., 2005). Total RNA was extracted from excised root tips (~5 mm apical segments) using an extraction kit (Plant RNeasy; Qiagen, Valencia, CA, USA). Genomic DNA was eliminated by treatment with RNase-free DNase I according to the manufacturer's instructions (Invitrogen, Carlsbad, CA, USA). The concentration of total RNA was measured by spectrophotometer, and 1 μg of total RNA was reverse-transcribed with the Superscript II Reverse Transcription Kit according to the manufacturer's instructions (Invitrogen). Efficiency for all primers is above 1.8, and sequences are given in Table S2 in the supplementary material. These primers all have a T_m of ~58°C. *ACTIN2* (*At3g18780*) or *UBQ10* (*At4g05320*) were used as reference genes. The cDNA was amplified using an appropriate kit (SYBR Green Master, containing Hot-Start Taq polymerase; Applied Biosystems). The cycling program was as follows: 10 minutes at 95°C, followed by 40 cycles of 30 seconds at 95°C, 1 minute at 57°C and 30 seconds at 72°C. To check the specificity of annealing of the oligonucleotides, melting curves were established at the end of the run between 55°C and 95°C and a ramping speed of 2°C per minute. Fluorescence data were acquired at the 72°C step and during the melting curve program. Relative transcript levels of the gene of interest were expressed as $2^{-\Delta Ct}$, where $-\Delta Ct$ is the difference in the number of cycles to the threshold between the gene of interest and the reference. In each run, at least three technical replicates were performed for each sample. The results presented are based on three independent biological replicates.

Flow cytometry

Flow cytometry was performed on a CyFlow flow cytometer running FloMax (Partec, Münster, Germany). Apical, 3-mm root-tip segments of 6-day-old seedlings were frozen and chopped with a razor blade and the homogenate filtered through 30-μm mesh as described previously (Boudolf et al., 2004), except that CyStain solution (Partec) replaced the extraction and staining solutions.

Microscopy and histology

Roots were embedded in butyl-methyl methacrylate and stained for tubulin and DNA as described (Baskin and Wilson, 1997). For whole-mount observations, roots were fixed and treated as described for microtubule observation (Bannigan et al., 2006). For labeling DNA and microtubules, after the secondary antibody, seedlings were rinsed in PBS and treated with 1 μg/ml RNase A for 1 hour at 37°C, followed by a PBS rinse and incubation in 3 μM propidium iodide for 1 hour at room temperature. Seedlings were rinsed again in PBS, root tips were excised and mounted in Prolong Gold (Invitrogen) and observed by confocal fluorescence microscopy (Zeiss Meta 510C). To score mitotic index, roots were fixed as described above and stained in 5 μg/ml 4,6-diamino-2-phenylindole dihydrochloride (DAPI) for 15 minutes, rinsed, mounted, and imaged with the 405 nm laser line of a Nikon Eclipse C1 confocal microscope.

To observe microtubules or chromosomes in living roots, GFP reporter lines were handled as described (Bannigan et al., 2006). To observe root apical meristem histology, seedlings were stained in growth medium containing 3 μM FM 4-64 dye (Invitrogen) for 5 to 10 minutes, then washed in growth medium briefly and examined under the Nikon confocal microscope. To quantify cortical microtubule alignment, roots of GFP-tubulin-expressing seedlings were imaged through the Nikon confocal microscope and projection images of epidermal cells obtained. The angle formed by the long axis of the root and microtubules was measured in Image J (http://rsbweb.nih.gov/ij/). Angles were binned in 10° increments between 0° and 90°, with angles between 90° and 180° taken as the supplementary angle. For each treatment, at least 400 microtubules were measured from five cells per root and between eight and 12 roots. For transmission electron microscopy, the method of Eleftheriou et al. was used (Eleftheriou et al., 2005).

GUS staining was performed on transgenic seedlings expressing a cyclin B1;1-GUS reporter construct (Colón-Carmona et al., 1999). Seedlings were incubated in cold acetone for 15 minutes, and then incubated in staining solution (100 mM sodium phosphate buffer pH 7.0, 10 mM EDTA, 0.5 mM potassium ferricyanide, 0.5 mM potassium ferrocyanide, 0.5% Triton X-100 and 2 mM X-glucuronide) at 37°C for 3 hours. Seedlings were washed three times with the above solution without the substrate, and then cleared according to Malamy and Benfey (Malamy and Benfey, 1997).

For the terminal transferase-mediated DNA end-labeling (TUNEL) assay, seedlings were fixed in 4% paraformaldehyde in PBS for 1 hour. Seedlings were digested in 0.1% pectinase and 0.01% pectolyase for 15 minutes, and

rinsed in 10% glycerol and 0.2% Triton X-100 for another 15 minutes. Wild-type seedlings treated with DNase I (200 U/ml) for 15 minutes were used as a positive control. TUNEL-positive nuclei were detected with the In Situ Cell Death Detection Kit (fluorescein) according to the manufacturer's protocol (Roche).

RESULTS

Positional cloning of *Arabidopsis thaliana RSW4*

To identify *RSW4*, we undertook positional cloning (see Fig. S1 in the supplementary material). We crossed *rsw4* onto the Landsberg *erecta* wild type and tested mutant seedlings in the F2 progeny for linkage to mapped polymorphic SSLP and CAPS markers. Based on 2304 chromosomes, *RSW4* was localized to a ~350 kb region between ciw32 and ciw44 on the bottom arm of chromosome 4. Then, additional markers narrowed the location to a 56 kb genomic segment that contains 12 annotated genes. To cover this region, we isolated a non-redundant set of seven cosmid clones by colony hybridization and multiplex PCR. The clones were transformed individually into *rsw4* and one of them (A1) complemented the mutant phenotype, with the F2 progeny showing a wild type to mutant segregation ratio of 3:1. The complementing cosmid contained two complete annotated gene sequences, *At4g22970* and *At4g22980*, which were absent (or incomplete) in the non-complementing cosmids. Sequencing genomic DNA revealed that in *rsw4*, there was a specific point mutation in the coding region of *At4g22970* that led to a missense mutation, whereas *At4g22980* was identical in *rsw4* and wild type. Therefore, we conclude that *At4g22970* is *RSW4*.

At4g22970 encodes a protein with homology to separase. This enzyme has been widely studied in animals and fungi and is a protease that cleaves the cohesin complex at the start of anaphase, thereby allowing sister chromatids to disjoin (Nasmyth et al., 2000). Recently, a reverse-genetics approach was used to study separase in *A. thaliana* (Liu and Makaroff, 2006). These authors showed that evidently null alleles containing T-DNA insertions in *At4g22970* give rise to embryo lethality. They also showed that decreasing the expression of this gene specifically in male meiotic cells, by means of a targeted RNAi construct, gave rise to the defective disjunction that is characteristic of a failure to remove cohesin. Because the function of separase was discovered in budding yeast, where the protein was named Extra Spindle Poles (Ciosk et al., 1998), we will refer to *At4g22970* as *AtESP*.

Defective chromosome disjunction at mitotic anaphase in *rsw4*

A hallmark of diminished separase function is aberrant chromosome disjunction. To investigate the status of chromosomes, we observed mitotic cells in root tips. Roots were fixed, stained with DAPI and examined in whole-mounts using the 405 nm laser line of the confocal microscope (Fig. 1A-D). In the wild type exposed to 30°C for 24 hours, chromosomes separated cleanly at anaphase (Fig. 1A). However, in *rsw4*, chromosome disjunction was anomalous. In some cells, disjoined and non-disjoined chromosomes were found in the same spindle (Fig. 1B); in other cells, chromosome fragments were present in aberrant configurations (Fig. 1C), often apparently numbering more than ten (the 4C chromosome number of this species) (Fig. 1D). To image chromosomes along with the mitotic spindle, roots were embedded in methacrylate, sectioned and double stained to show DNA and microtubules (Fig. 1E-L). In roots exposed to 30°C for 14 hours, *rsw4* cells in metaphase could not be distinguished from those of the wild type (not shown) or from *rsw4* maintained at 19°C (Fig. 1E,I versus 1F,J). In anaphase or telophase, bridges linking separated chromatin masses or nuclei were not seen in wild-type cells at 30°C (Fig. 1G,K), whereas they were common in *rsw4* at this temperature (Fig. 1H,L). These defects are typical of separase-deficient eukaryotes, and confirm the molecular identification of *RSW4* as *AtESP*.

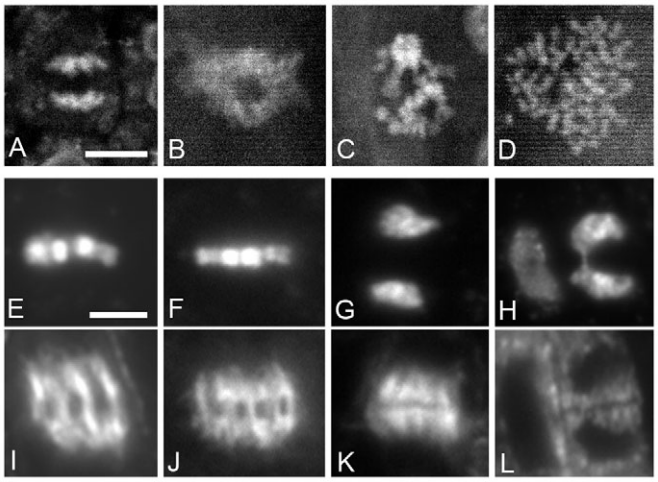

Fig. 1. Chromatin and microtubules in root mitotic cells. (**A-D**) Confocal micrographs of whole-mounts stained with DAPI to show DNA. Seven-day-old wild-type (A) and *rsw4* (B-D) *Arabidopsis thaliana* seedlings were transferred to 30°C for 24 hours before fixation. Note the aberrant disjunction and chromosome fragmentation. (**E-L**) Wide-field micrographs of methacrylate sections double stained to show DNA (E-H) and microtubules (I-L). Seven-day-old seedlings were maintained at 19°C or transferred to 30°C for 14 hours before fixation. (E,I) *rsw4* metaphase, 19°C. (F,J) *rsw4* metaphase, 30°C. (G,K) Wild-type telophase, 30°C. (H,L) *rsw4* telophase, 30°C. Note the chromatin bridge linking telophase nuclei in *rsw4* (L). Scale bars: 5 μm.

Because mitotic figures examined in sections can often be ambiguous, we used whole-mount preparations stained for tubulin and DNA (with propidium iodide) and observed by confocal fluorescence microscopy (Fig. 2). Again, roots were exposed to 30°C for 14 hours prior to fixation. In *rsw4* cells at telophase, chromosome bridges were common, as were mitotic cells with apparently more than ten chromosomes (not shown). In some *rsw4* cells, chromatin masses appeared to interrupt a forming cell wall or to be stuck to the forming cell wall (Fig. 2A-C). Interestingly, a pair of spindles sometimes formed adjacent to a common cell wall (Fig. 2D), as if daughter nuclei had remained anchored to the new cell wall until entering mitosis again. Neither type of formation was observed in the wild type. Although the arrangement of chromatin in *rsw4* was commonly aberrant, microtubule organization in spindles and phragmoplasts appeared similar to that of the wild type, in both methacrylate sections (Fig. 1) and whole-mounts (Fig. 2).

To evaluate the penetrance of aberrant chromosome disjunction, roots were fixed and stained with DAPI and examined in whole-mounts. With optical sectioning, metaphase and anaphase division figures could be found throughout the root. In the wild type at either temperature, and in *rsw4* at 19°C, almost half of such figures were in metaphase, and among cells in anaphase only a few were scored as abnormal (Table 1). With *rsw4* at 30°C for only 2 hours, the percentage of metaphase division figures grew modestly, whereas that of abnormal anaphase figures grew substantially. By 24 hours at 30°C, nearly all of the anaphase figures in *rsw4* roots appeared to

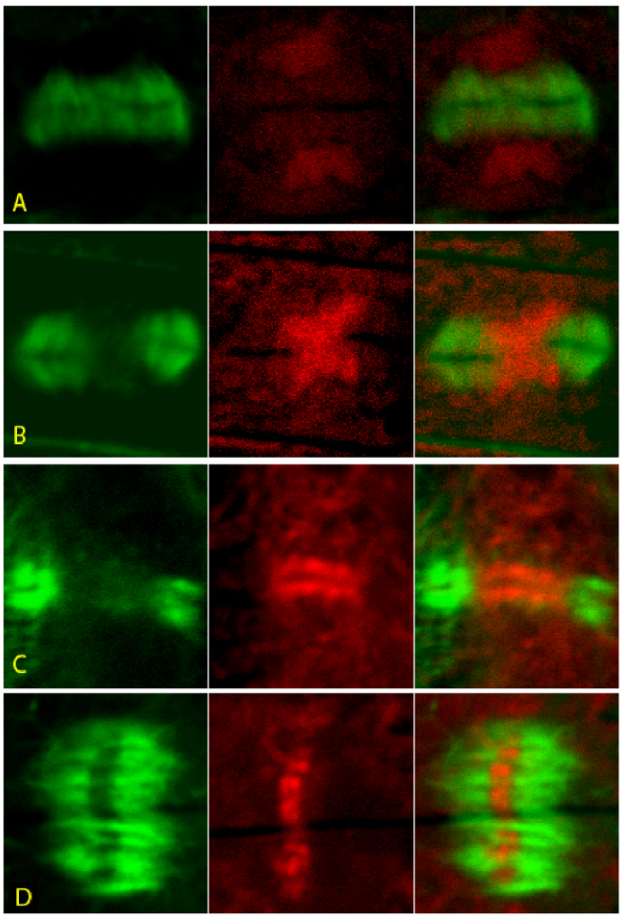

Fig. 2. Chromatin and microtubules in root mitotic cells imaged in whole-mounts by confocal fluorescence microscopy. (**A-D**) Staining of microtubules (green, left) and nucleic acid (red, center), with merged images shown to the right. Seven-day-old wild-type (A) and *rsw4* (B-D) seedlings were transferred to 30°C for 14 hours before fixation. Note chromatin at the position of the cell plate (B,C) and a large mitotic spindle appearing to straddle a cell wall (D) in *rsw4*.

be aberrant. These data show that transfer of *rsw4* to the restrictive temperature rapidly and pervasively interrupts chromosome disjunction in the root.

To gain further insight into the defective chromosome separation we used GFP reporters. We crossed *rsw4* onto a line expressing tubulin-GFP and onto a line expressing histone H3.3-GFP. In both metaphase and anaphase, mitotic spindles appeared indistinguishable in the two genotypes and at the two temperatures (see Movies 1, 2 in the supplementary material). This confirms the inference from the fixed cells that the *rsw4* phenotype does not include defective mitotic spindles. In contrast to microtubules, chromosome movement in *rsw4* was aberrant. In the wild type, metaphase cells commonly entered anaphase, which took ~2 minutes to complete (Fig. 3A; see Movie 3 in the supplementary material). By contrast, in *rsw4* seedlings exposed to 30°C for only 3 hours, anaphase was prolonged. In some cells, chromosomes on a metaphase plate initiated anaphase but did not separate completely (Fig. 3B). However, in most cells, chromosome masses were found that appeared to comprise incompletely segregated chromosomes, which remained so during the period of observation (Fig. 3C,D; see Movies 4, 5 in the supplementary material).

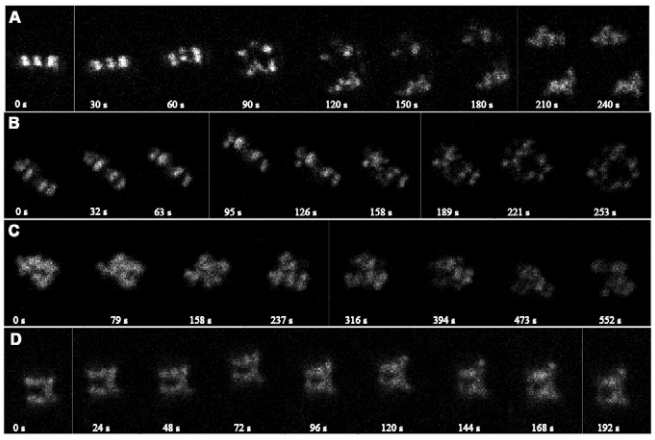

Fig. 3. Stills from time-lapse images of roots expressing histone H3-GFP and imaged by confocal fluorescence microscopy. Time in seconds is shown below each image. Seedlings were maintained at 30°C during imaging. (**A**) Wild type exposed to 30°C for ~14 hours prior to imaging. Anaphase begins before 60 seconds and is complete by 180 seconds, a timing that is typical of wild-type mitosis. Stills are from Movie 3 in the supplementary material. (**B-D**) *rsw4* exposed to 30°C. No examples (0/10) were recorded of complete segregation of chromosomes. (B) *rsw4* at 30°C for 30 minutes. Anaphase initiates (158 seconds) but disjunction is incomplete. (C) *rsw4* at 30°C for 1.5 hours. Metaphase-like chromosomes remain clustered in the cell center for the entire sequence (552 seconds). Stills are from Movie 4 in the supplementary material. (D) *rsw4* at 30°C for 3 hours. Anaphase has initiated but a large chromatin bridge appears and segregation is inhibited. Stills are from Movie 5 in the supplementary material.

Cell production rate at the permissive temperature

At the permissive temperature, although *rsw4* roots do not swell, they elongate more slowly than wild-type roots (Wiedemeier et al., 2002). However, the chromosome disjunction anomalies reported above were rare at the permissive temperature, suggesting additional effects of the *rsw4* mutation. To investigate cell division, we quantified cell production rate, which represents the total output of cells per file of a given tissue with time (Rahman et al., 2007). Note that this assay for cell production rate assumes steady state behavior and hence cannot be applied to roots at the restrictive temperature

Table 1. Relative frequencies of metaphase and anaphase in wild-type and *rsw4* roots

Treatment	Metaphase (%)	Normal anaphase (%)	Abnormal anaphase (%)
Wild type			
19°C	40 ± 2	55 ± 2	5 ± 1
30°C, 24 hours	38 ± 3	56 ± 3	6 ± 2
rsw4			
19°C	38 ± 4	57 ± 5	5 ± 1
30°C, 2 hours	50 ± 7	16 ± 9	34 ± 8
30°C, 12 hours	58 ± 4	7 ± 3	35 ± 2
30°C, 24 hours	38 ± 14	5 ± 3	57 ± 13

Roots were fixed at the times indicated and stained for DNA with DAPI and examined by confocal fluorescence microscopy. Data are mean ± s.d. for six to 14 roots; expressed as a percentage of the total number of anaphases and metaphases for each treatment. Abnormal anaphase indicates lagging chromosomes; bridges; and other patterns of unusual segregation; and might include some cells in prometaphase as well as in early telophase.

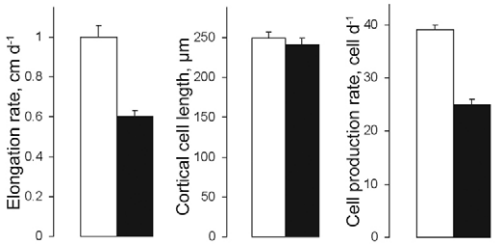

Fig. 4. Growth parameters of roots at the permissive temperature. Wild-type (white) and *rsw4* (black) seedlings were grown at 19°C for 7 days. Root elongation rate was measured over the final 24-hour period and then the lengths of 20 mature cortical cells were measured per root. Cell production rate was calculated as the ratio of elongation rate to cell length for each root. Bars show mean ± s.e.m. of three replicate experiments. Note that the root elongation rate in *rsw4* at 19°C decreases by about the same extent as the cell production rate. d, day.

because their growth changes steeply over time. The slowed elongation at 19°C involved no significant decrease in cell length and hence a substantial decrease in cell production rate (Fig. 4). This implies that the decreased elongation rate of *rsw4* at 19°C results from defects in cell division rather than in expansion. Consistently, direct measurement of maximal expansion rate within the elongation zone revealed no difference between *rsw4* and the wild type (data not shown).

Cell cycle analysis

To determine whether the cell cycle becomes arrested in *rsw4*, we first used flow cytometry (Fig. 5). Exposure of the wild type to 30°C for 24 hours caused no detectable change in the distribution of DNA content among root tip nuclei. In *rsw4* at 19°C, ~2% of nuclei had reached 32C, whereas in the wild type, nuclei with 32C levels were undetectable. For *rsw4* at 30°C, ploidy tended to increase further, which might reflect a contribution from nuclei formed following non-disjunction. However, the number of nuclei with 2C or 4C DNA content tended to decrease, a trend that is inconsistent with cell cycle arrest at a specific checkpoint.

To assess the cell cycle further, we used quantitative real-time RT-PCR (qRT-PCR) to measure the steady state transcript level for genes known to be regulated transcriptionally during the cell cycle (Menges et al., 2005). To enrich for proliferating cells, RNA was obtained from 5-mm apical root-tip segments. RNA was extracted 12 hours after transfer to 30°C, which is after a period of significant disturbance to mitosis but precedes detectable root swelling. With just one exception, marker expression was little affected (Fig. 6), confirming the lack of cell cycle arrest inferred from flow cytometry.

The exception was a histone H4 transcript, which decreased by ~60%. However, out of more than 40 histone genes subsequently assayed (see Table S3 in the supplementary material), the expression of only two changed more than twofold (one H1 decreased by 50% and one H3.2 doubled). Furthermore, these three histone transcripts changed in *rsw7*, a mutant with defective mitosis caused by a mutation in a kinesin (Bannigan et al., 2007). Insofar as histone genes are all transcriptionally upregulated in S phase (Marzluff and Duronio, 2002), these results substantiate our conclusion that the cell cycle is not arrested in *rsw4* and indicate that the H4 marker originally chosen (*At5g59970*) behaved anomalously.

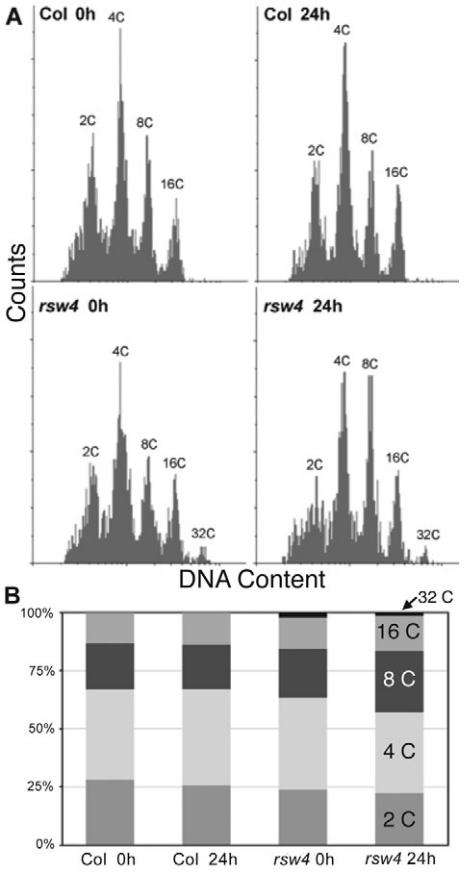

Fig. 5. Flow cytometric analysis of DNA content. (**A**) Representative DNA content distributions. For each sample, ~2000 nuclei were measured. Note the increase of the 8C DNA population in the *rsw4* mutant upon transferring to the restrictive temperature. (**B**) Quantification of the data represented in A. The data represent the average of two biologically independent experiments.

Polarity, microtubules and cyclin B

Along with radial swelling, the orientation of cell division is altered in *rsw4*, perturbing histology (Wiedemeier et al., 2002). Although phragmoplasts and preprophase bands formed in the mutant with evidently wild-type structure, aberrant chromosome masses interfered with cell plate formation (see Fig. S2 in the supplementary material). Cell walls were often completely or partially interrupted by a nucleus. When cells had multiple chromatin masses after anaphase, several phragmoplasts formed, leading to wandering cell walls at unusual orientations. It remains to be determined whether these hindrances to cell wall construction are sufficient to explain the altered histology seen in the mutant or if there are additional disturbances to organ polarity.

A sensitive indicator of organ polarity are the cortical microtubules, which in most of the *A. thaliana* root growth zone are strictly transverse to the long axis of the root. Root diameter in *rsw4* diverged from that of the wild type, starting 15 hours after exposure to the restrictive temperature (Fig. 7A). In living root epidermal cells expressing GFP-tubulin, cortical microtubules in the wild type retained their principally transverse orientation, but those of the mutant were often disorganized (Fig. 7B-D). The disorganization seen in these images was confirmed by measuring microtubule angles, which revealed a progressive disorganization with time

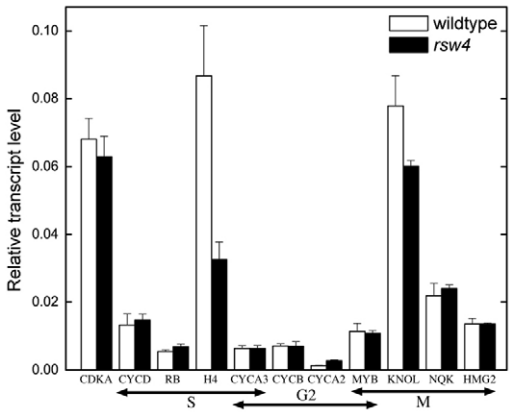

Fig. 6. Relative transcript levels of selected cell cycle genes. Seven-day-old seedlings were transferred to 30°C for 12 hours and RNA was extracted from 5 mm apical segments of the root. Transcript levels were measured with respect to *ACTIN2* (*At3g18780*). Bars show mean ± s.e.m. of three biological replicates with technical replicates for each RNA sample. Assayed genes are as follows (for gene numbers and primer sequences, see Table S2 in the supplementary material): *CDKA*, *CYCLIN-DEPENDENT KINASE A* (expressed constitutively); *CYCD*, *CYCLIN D3;1*; *RB*, *RETINOBLASTOMA-RELATED PROTEIN*; *H4*, *HISTONE H4*; *CYCA3*, *CYCLIN A3;1*; *CYCB*, *CYCLIN B1;1*; *CYCA2*, *CYCLIN A2;1*; *MYB*, *MYB3-R4*; *KNOL*, *KNOLLE*; *NQK*, *NQK1* (*MAP KINASE 6*); *HMG2*, a gene found to be specifically expressed in M phase (Fredrik Coppens, Flanders Institute for Biotechnology (V.I.B.) Ghent University, personal communication).

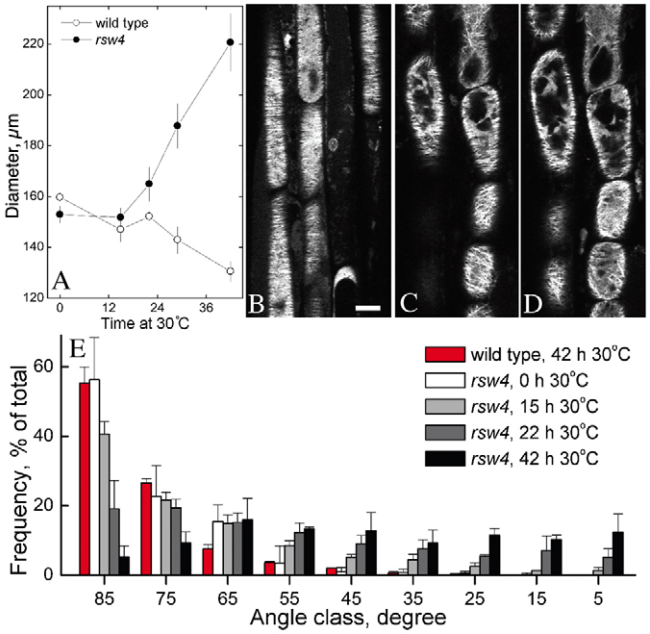

Fig. 7. Radial swelling and cortical microtubule organization. (**A**) Seven-day-old wild-type and *rsw4* seedlings were transferred to 30°C at time zero and root diameter measured at the indicated times. The mean of three replicate experiments ± s.e.m. is plotted. The gradual thinning of the wild type is consistent with the decreased elongation rate over that period. Note the onset of radial expansion in *rsw4* at ~15 hours. (**B-D**) Cortical microtubules in living root epidermal cells expressing GFP-β-tubulin 6 and exposed to 30°C for 22 hours after 7 days at 19°C. Microtubules are generally transverse to the long axis of the root in the wild type (B), but less well organized in *rsw4* (C,D, which show two different focal planes for clarity). Scale bar: 10 μm. (**E**) Distribution of microtubule angle for cortical microtubules imaged as in C,D. Distributions reflect several hundred microtubules each. The distribution of microtubules for wild type at 19°C closely resembles that shown for the wild type at 42 hours and 30°C.

(Fig. 7E). Microtubule disorganization was concomitant with swelling and underscores the defective polarity of the mutant root, at least after 15 hours of the loss of separase function.

Several mutants have been identified in which disruption of organ polarity is associated with ectopic accumulation of cyclin B1;1 (Suzuki et al., 2005; Inagaki et al., 2006; Zhu et al., 2006). We therefore crossed *rsw4* into a line that harbors a widely used cyclin B1;1 reporter (Colón-Carmona et al., 1999). In this reporter, GUS is driven from the native promoter and is translationally fused to an N-terminal portion of the protein that contains the signal for degradation (the D-box). In wild-type cells, GUS expression is punctate, reflecting the cells that happened to have been in G2/M at the time of staining (Fig. 8A). A similar pattern was seen in wild-type seedlings transferred to 30°C for 24 hours and in *rsw4* at 19°C (Fig. 8B,C). However, the staining dramatically increased in *rsw4* as a function of time at 30°C (Fig. 8D-F). Staining was constant for *rsw4* expressing the auxin reporter DR5-GUS (Sabatini et al., 1999) (not shown), arguing against a change in oxidation state that enhances the reaction rate of the glucuronidase. Because the mRNA level for *CYCB1;1* was little affected at 12 hours (Fig. 6), it appears that the pronounced increase in GUS staining reflects a failure to degrade the protein.

DNA damage responses

Ectopic accumulation of cyclin B1;1, as well as root swelling, can be caused by DNA damage (Culligan et al., 2004). We therefore determined to what extent DNA damage, or a response thereto, occurred in *rsw4*. First, we compared dose-response curves between wild type and *rsw4* for hydroxyurea and mutagenic ultraviolet (250 nm) and found no significant differences between the genotypes (data not shown), including experiments at the permissive temperature, where the decrease in cell production (Fig. 4) indicates partial loss of separase function. Separase has been implicated in DNA repair (Nagao et al., 2004; Sak et el., 2008) and non-disjunction itself damages DNA. To assay double-stranded DNA breakage directly, we used the TUNEL assay. Although TUNEL-positive nuclei were easily detected in the DNase I control, nuclei in *rsw4* were not labeled above background (Fig. 9A-C), suggesting that widespread DNA damage was absent. Finally, we examined the expression of three genes, *WEE1*, *RAD51* and *PARP2*, the expression of which is known to be strongly increased in response to DNA damage (De Schutter et al., 2007). Expression of these genes was scarcely affected in *rsw4* (Fig. 9B). Taken together, it appears that *rsw4* has an essentially undisturbed response to DNA damage.

DISCUSSION

Separase and chromosome disjunction

This work identifies *RSW4* as *AtESP*, the *A. thaliana* homolog of separase. This identification is based on molecular analysis, as well as on the loss-of-function phenotype of *rsw4* having defective chromosome disjunction, as invariably reported for separase mutants, including in *A. thaliana* when RNAi was used to downregulate *AtESP* in meiocytes (Liu and Makaroff, 2006; Yang et al., 2009). Indeed, meiocytes of *rsw4* plants transferred to 30°C closely resemble those in which separase expression is decreased

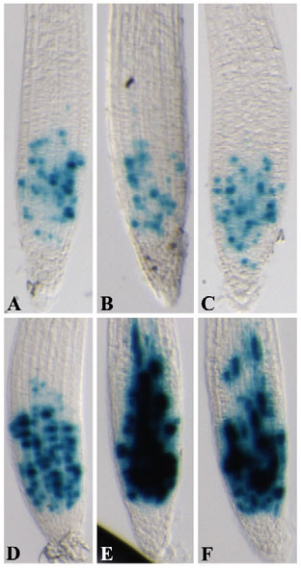

Fig. 8. Expression of cyclin B1;1-GUS. Roots were 7 days old at the start of the experiments. (**A**) Wild type at 19°C. (**B**) Wild type at 30°C for 24 hours. (**C**) *rsw4* at 19°C. (**D**) *rsw4* at 30°C for 9 hours. (**E**,**F**) *rsw4* at 30°C for 24 hours.

with RNAi (data not shown). A genomic fragment containing *AtESP* complemented the growth and division phenotypes of *rsw4*. An ambiguity exists for the latter result insofar as the complementing clone contained a small open reading frame upstream of the separase. However, this gene in *rsw4* had a wild-type sequence, and its expression was neither altered in *rsw4* nor, based on community resources, associated with dividing tissues. Taken together, these results indicate that *RSW4* is *AtESP*.

This work adds mitosis in a seed plant to the list of eukaryotic cell types in which separase has been shown to be responsible for allowing sister chromatids to disjoin. Although this might be expected, the result is not a foregone conclusion. Plants have diverged from animals and fungi for hundreds of millions of years and have accumulated differences in their machinery for cell division. Dynein plays a leading role in the mitosis of animals and fungi but has been lost entirely from flowering plants. A regulator of separase called securin is essential in yeast (Onn et al., 2008), but is almost, although not quite, dispensable in mice (Kumada et al., 2006; Wirth et al., 2006) and, based on sequence similarity, is absent from plant genomes. The forms of chromosome disjunction in *rsw4* closely resemble those of other eukaryotes with defective separase and substantiate our conclusion of conserved function.

Separase and the cell cycle

The cell cycle bristles with regulatory spines to block untimely proliferation; in view of this, one might find the lack of cell cycle arrest in *rsw4* at the restrictive temperature surprising. Nevertheless, cells appear to lack a checkpoint that monitors disjunction per se. In general, defects in disjunction, as caused by separase deficiency and examined in a wide variety of taxa, occur with continued proliferation, allowing highly polyploid cells to accumulate, often with two (or four or more) replicated chromosomes remaining bound together at the centromeres (Jäger et al., 2001; Siomos et al., 2001; Kumada et al., 2006; Wirth et al., 2006). This phenotype is inconsistent with cell cycle arrest and resembles that shown here for *rsw4* (Fig. 1).

In *rsw4*, the accumulation of cyclin B1;1 could be interpreted as evidence for a G2/M arrest; however, there was no concomitant increase in the *CYCB1;1* mRNA, which would be expected for a checkpoint-driven delay. Furthermore, when overexpressed on its own, cyclin B does not invariably block the cell cycle (Amon et al., 1994; Cross et al., 1999; Criqui et al., 2000).

The clearest example of separase deficiency disturbing the cell cycle is found in yeast, in which separase helps to regulate exit from M phase through its interactions with a regulatory phosphatase (Stegmeier et al., 2002; Sullivan and Uhlmann, 2003). Separase also helps regulate exit from M phase in oocytes, although using a different pathway (Terret and Jallepalli, 2006), but usually not in mitotic cells, with the exception of zebrafish embryos (Shepard et al., 2007). By contrast, delays entering mitosis occur in separase-deficient human cell lines (Sak et al., 2008), and these delays are associated with defective spindle assembly and chromosome alignment (Giménez-Abián et al., 2005; Papi et al., 2005). However, neither undue delays at G2/M nor defective spindles accompany separase deficiencies in whole animals and in certain other cell lines (Jäger et al., 2001; Siomos et al., 2001; Padney et al., 2005; Kumada et al., 2006; Wirth et al., 2006). For somatic animal cells, these observations argue against a substantial role for separase in regulating cell cycle progression.

Indications that AtESP is involved in cell cycle regulation, although not at a specific checkpoint, come from *rsw4* phenotypes at the permissive temperature. In *rsw4* at 19°C, there was little or no cytological evidence of chromosome non-disjunction, indicating that the phenotypes seen reflect other activities of the separase. First,

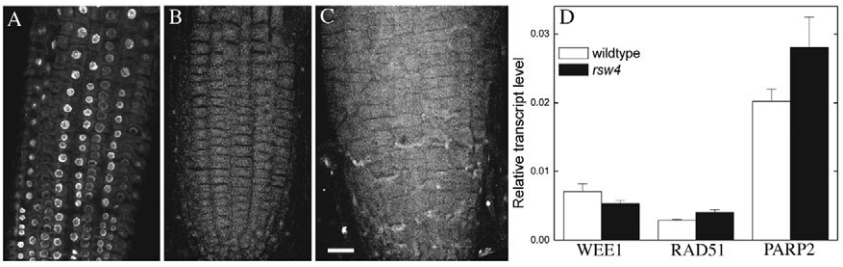

Fig. 9. DNA damage and response. (**A-C**) TUNEL assay for double-strand DNA breakage. (A) Wild-type root treated with DNase I for 30 minutes (positive control). (B) Wild type. (C) *rsw4*. For B and C, roots were exposed to 30°C for 24 hours. Scale bar: 10 μm. (**D**) Relative transcript levels in wild type and *rsw4*, as measured by qRT-PCR, for three genes (*WEE1*, *RAD51*, *PARP2*) that are regulated transcriptionally in response to DNA damage. Transcripts were measured with respect to *ACTIN2* (*At3g18780*). Bars show mean ± s.e.m. of three replicate RNA extractions with technical replicates for each RNA sample.

cell production rate at 19°C was ~65% of that of the wild type (Fig. 4), a reduction that is consistent with reduced numbers of division figures found in DAPI-stained roots (data not shown). Second, *rsw4* roots had a population of nuclei with a 32C DNA level (Fig. 5), which is a level rarely, if ever, attained in wild-type roots (Boudolf et al., 2004; Ramirez-Parra et al., 2004; Imai et al., 2006; Anonymous, 2009). Together, these phenotypes imply a role for separase in the cell cycle transition from proliferation to endoreduplication.

Separase, organ polarity and cyclin B1;1

The *rsw4* mutant was identified through its swollen root, but the identification of RSW4 as separase (AtESP) offered no explanation for this altered morphology. To account for swelling, one must examine elements that regulate cell wall anisotropy, such as the cortical array of microtubules. In the original characterization of *rsw4* (Wiedemeier et al., 2002), cortical microtubules were reported to be unaffected, but we show here that they become disorganized, concomitant with root swelling. The reason for the discrepancy is not clear; however, Wiedemeier et al. used plastic sections, which sample the cortical array only in small, irregular patches, and looked for large disruptions, as occur with inhibitors. This was recently argued by Bannigan et al. (Bannigan et al., 2007), who found disorganized cortical microtubules in *rsw7*, a mutant that Wiedemeier et al. also reported to have unaffected microtubules. Disorganized microtubules in *rsw4* account for root swelling. The question now becomes: what links microtubules to separase function.

We suggest that the link is cyclin B1;1. This cyclin accumulates in several backgrounds that are defective in genome structure and chromatin maintenance (Suzuki et al., 2005; Inagaki et al., 2006; Zhu et al., 2006) or in response to DNA damage (De Schutter et al., 2007), in some cases only in the presence of DNA-damaging agents (Culligan et al., 2004; Hefner et al., 2006). In all these backgrounds, the superabundant cyclin is associated with some degree of altered histology and often root swelling. In transgenic tobacco expressing a non-degradable version of cyclin B1;1 (Weingartner et al., 2004), as well as in the *hobbit* mutant of *A. thaliana*, which reduces the function of the complex responsible for degrading cyclin B1;1 (Serralbo et al., 2006), cortical microtubules are disorganized and to a similar extent as reported here for *rsw4*. Although the original study overexpressing cyclin B1 in tobacco BY-2 cells reported wild-type morphology (Criqui et al., 2000), a subsequent study found that higher expression levels are needed to provoke microtubule disorganization and altered cell shape (Weingartner et al., 2004). This suggests that among mutants with ectopic cyclin B1;1 accumulation, those with root swelling have higher levels of cyclin B1;1 expression than those without, and that in *rsw4*, ~15 hours are needed for levels to accumulate sufficiently to alter microtubules and hence morphology.

Thus, many observations fit with the idea that accumulating cyclin B1;1 disrupts cortical microtubules. But what is the connection between the cyclin and separase? The mutants cited above all involve chromatin maintenance, which is a separase function, and separase loss-of-function can damage DNA, as non-separated chromosomes are pulled apart on the mitotic spindle. Also, separase has been reported to be active in DNA repair (Nagao et al., 2004). Hence, in *rsw4*, DNA damage could be responsible for driving up cyclin B1;1 levels. However, we failed to obtain evidence that DNA damage responses are impaired in *rsw4*, finding neither cell cycle arrest, TUNEL-positive nuclei, altered sensitivity to DNA-damaging agents, nor alteration of message levels of three pivotal regulators.

Instead, separase might be linked to cyclin B1;1 directly. In animals, one way that separase is regulated is through binding cyclin B1, as part of the CDK complex (Gorr et al., 2005; Holland and Taylor, 2006; Boos et al., 2008). This interaction has been viewed in terms of cyclin B negatively regulating separase. At the onset of anaphase, separase is activated via the proteolysis of its inhibitors, including cyclin B1, a proteolysis that is initiated by the anaphase-promoting complex. It is tempting to speculate that once active, separase itself helps to ensure the swift destruction of cyclin B. Separase mutants of yeast (Tinker-Kulberg and Morgan, 1999) and *Drosophila* embryos (Padney et al., 2005) accumulate excess cyclin B at metaphase. This accumulation, whatever its mechanism, points to a novel function for separase, and one of importance given how profoundly too much cyclin B1;1 disturbs plant morphogenesis.

Acknowledgements

We thank Abidur Rahman (now at Iwate University) for establishing the TUNEL assay; Alex Bannigan (now at James Madison University) for help with confocal fluorescence microscopy; Keith Earley and Craig Pikaard (Indiana University) for the GFP-histone line; Chris Makaroff (Miami University of Ohio) for sharing unpublished data on *rsw4* meiocytes; and Frederik Coppens [Flanders Institute for Biotechnology (V.I.B.) Ghent University] for unpublished data on HMG2. L.D.V. is a postdoctoral fellow of the Research Foundation-Flanders. This work was supported in part by the Max-Planck Society (W.-R.S. and D.S.), and by a grant from the US Department of Energy (DE-FG02 03ER15421 to T.I.B.), which does not constitute endorsement by that department of views expressed herein.

Competing interests statement

The authors declare no competing financial interests.

Supplementary material

Supplementary material for this article is available at
http://dev.biologists.org/lookup/suppl/doi:10.1242/dev.041939/-/DC1

References

Amon, A., Irniger, S. and Nasmyth, K. (1994). Closing the cell cycle circle in yeast: G2 cyclin proteolysis initiated at mitosis persists until the activation of G1 cyclins in the next cycle. *Cell* **77**, 1037-1050.

Anonymous (2009). http://www.biocompare.com/Articles/ApplicationNote/1704/Simultaneous-Analysis-of-GFP-Transgene-Expression-and-Plant-Cell-Ploidy-With-the-Accuri-C6-Cytometer-System.html

Bannigan, A., Wiedemeier, A. M., Williamson, R. E., Overall, R. L. and Baskin, T. I. (2006). Cortical microtubule arrays lose uniform alignment between cells and are oryzalin resistant in the arabidopsis mutant, *radially swollen 6*. *Plant Cell Physiol.* **47**, 949-958.

Bannigan, A., Scheible, W. R., Lukowitz, W., Fagerstrom, C., Wadsworth, P., Somerville, C. and Baskin, T. I. (2007). A conserved role for kinesin-5 in plant mitosis. *J. Cell Sci.* **120**, 2819-2827.

Baskerville, C., Segal, M. and Reed, S. I. (2008). The protease activity of yeast separase (esp1) is required for anaphase spindle elongation independently of its role in cleavage of cohesin. *Genetics* **178**, 2361-2372.

Baskin, T. I. and Wilson, J. E. (1997). Inhibitors of protein kinases and phosphatases alter root morphology and disorganize cortical microtubules. *Plant Physiol.* **113**, 493-502.

Bembenek, J. N., Richie, C. T., Squirrell, J. M., Campbell, J. M., Eliceiri, K. W., Poteryaev, D., Spang, A., Golden, A. and White, J. G. (2007). Cortical granule exocytosis in *C. elegans* is regulated by cell cycle components including separase. *Development* **134**, 3837-3848.

Boos, D., Kuffer, C., Lenobel, R., Korner, R. and Stemmann, O. (2008). Phosphorylation-dependent binding of cyclin B1 to a Cdc6-like domain of human separase. *J. Biol. Chem.* **283**, 816-823.

Boudolf, V., Vlieghe, K., Beemster, G. T. S., Magyar, Z., Torres Acosta, J. A., Maes, S., Van Der Schueren, E., Inzé, D. and De Veylder, L. (2004). The plant-specific cyclin-dependent kinase CDKB1;1 and transcription factor E2Fa-DPa control the balance of mitotically dividing and endoreduplicating cells in Arabidopsis. *Plant Cell* **16**, 2683-2692.

Ciosk, R., Zachariae, W., Michaelis, C., Shevchenko, A., Mann, M. and Nasmyth, K. (1998). An ESP1/PDS1 complex regulates loss of sister chromatid cohesion at the metaphase to anaphase transition in yeast. *Cell* **93**, 1067-1076.

Clough, S. J. and Bent, A. F. (1998). Floral dip: a simplified method for Agrobacterium-mediated transformation of *Arabidopsis thaliana*. *Plant J.* **16**, 735-743.

Colón-Carmona, A., You, R., Haimovitch-Gal, T. and Doerner, P. (1999). Technical advance: spatio-temporal analysis of mitotic activity with a labile cyclin-GUS fusion protein. *Plant J.* **20**, 503-508.
Criqui, M. C., Parmentier, Y., Derevier, A., Shen, W. H., Dong, A. and Genschik, P. (2000). Cell cycle-dependent proteolysis and ectopic overexpression of cyclin B1 in tobacco BY2 cells. *Plant J.* **24**, 763-773.
Cross, F. R., Yuste-Rojas, M., Gray, S. and Jacobson, M. D. (1999). Specialization and targeting of B-type cyclins. *Mol. Cell* **4**, 11-19.
Culligan, K., Tissier, A. and Britt, A. (2004). ATR regulates a G2-phase cell-cycle checkpoint in *Arabidopsis thaliana*. *Plant Cell* **16**, 1091-1104.
Czechowski, T., Bari, R. P., Stitt, M., Scheible, W. R. and Udvardi, M. K. (2004). Real-time RT-PCR profiling of over 1400 Arabidopsis transcription factors: unprecedented sensitivity reveals novel root- and shoot-specific genes. *Plant J.* **38**, 366-379.
Czechowski, T., Stitt, M., Altmann, T., Udvardi, M. K. and Scheible, W. R. (2005). Genome-wide identification and testing of superior reference genes for transcript normalisation in *Arabidopsis thaliana*. *Plant Physiol.* **139**, 5-17.
De Schutter, K., Joubes, J., Cools, T., Verkest, A., Corellou, F., Babiychuk, E., Van der Schueren, E, Beeckman. T., Kushnir, S., Inzé, D. et al. (2007). Arabidopsis WEE1 kinase controls cell cycle arrest in response to activation of the DNA integrity checkpoint. *Plant Cell* **19**, 211-225.
Eleftheriou, E. P., Baskin, T. I. and Hepler, P. K. (2005). Aberrant cell plate formation in the *Arabidopsis thaliana microtubule organization 1* mutant. *Plant Cell Physiol.* **46**, 671-675.
Giménez-Abián, J. F., Díaz-Martinez, L. A., Waizenegger, I. C., Giménez-Martín, G. and Clarke, D. J. (2005). Separase is required at multiple pre-anaphase cell cycle stages in human cells. *Cell Cycle* **4**, 1576-1584.
Gorr, I. H., Boos, D. and Stemmann, O. (2005). Mutual inhibition of separase and Cdk1 by two-step complex formation. *Mol. Cell* **19**, 135-141.
Hefner, E., Huefner, N. and Britt, A. B. (2006). Tissue-specific regulation of cell-cycle responses to DNA damage in arabidopsis seedlings. *DNA Repair* **5**, 102-110.
Higuchi, T. and Uhlmann, F. (2005). Stabilization of microtubule dynamics at anaphase onset promotes chromosome segregation. *Nature* **433**, 171-176.
Holland, A. J. and Taylor, S. S. (2006). Cyclin-B1-mediated inhibition of excess separase is required for timely chromosome disjunction. *J. Cell Sci.* **119**, 3325-3336.
Imai, K. K., Ohashi, Y., Tsuge, T., Yoshizumi, T., Matsui, M., Oka, A. and Aoyama, T. (2006). The A-type cyclin CYCA2;3 is a key regulator of ploidy levels in arabidopsis endoreduplication. *Plant Cell* **18**, 382-396.
Inagaki, S., Suzuki, T., Ohto, M. A., Urawa, H., Horiuchi, T., Nakamura, K. and Morikami, A. (2006). Arabidopsis TEBICHI, with helicase and DNA polymerase domains, is required for regulated cell division and differentiation in meristems. *Plant Cell* **18**, 879-892.
Jäger, H., Herzig, A., Lehner, C. F. and Heidmann, S. (2001). Drosophila separase is required for sister chromatid separation and binds to PIM and THR. *Genes Dev.* **15**, 2572-2584.
Kumada, K., Yao, R., Kawaguchi, T., Karasawa, M., Hoshikawa, Y., Ichikawa, K., Sugitani, Y., Imoto, I., Inazawa, J., Sugawara, M. et al. (2006). The selective continued linkage of centromeres from mitosis to interphase in the absence of mammalian separase. *J. Cell Biol.* **172**, 835-846.
Liu, Z. and Makaroff, C. A. (2006). Arabidopsis separase AESP is essential for embryo development and the release of cohesin during meiosis. *Plant Cell* **18**, 1213-1225.
Lukowitz, W., Gillmor, C. S. and Scheible, W.-R. (2000). Positional cloning in arabidopsis. Why it feels good to have a genome initiative working for you. *Plant Physiol.* **123**, 795-805.
Malamy, J. E. and Benfey, P. N. (1997). Organization and cell differentiation in lateral roots of *Arabidopsis thaliana*. *Development* **124**, 33-44.
Marzluff, W. F. and Duronio, R. J. (2002). Histone mRNA expression: multiple levels of cell cycle regulation and important developmental consequences. *Curr. Opin. Cell Biol.* **14**, 692-699.
Menges, M., de Jager, S. M., Gruissem, W. and Murray, J. A. (2005). Global analysis of the core cell cycle regulators of arabidopsis identifies novel genes, reveals multiple and highly specific profiles of expression and provides a coherent model for plant cell cycle control. *Plant J.* **41**, 546-566.
Meshi, T., Taoka, K. I. and Iwabuchi, M. (2000). Regulation of histone gene expression during the cell cycle. *Plant Mol. Biol.* **43**, 643-657.
Meyer, K., Leube, M. P. and Grill, E. (1994). A protein phosphatase 2C involved in ABA signal transduction in *Arabidopsis thaliana*. *Science* **264**, 1452-1455.
Nagao, K., Adachi, Y. and Yanagida, M. (2004). Separase-mediated cleavage of cohesin at interphase is required for DNA repair. *Nature* **430**, 1044-1048.
Nasmyth, K., Peters, J. M. and Uhlmann, F. (2000). Splitting the chromosome: cutting the ties that bind sister chromatids. *Science* **288**, 1379-1385.
Onn, I., Heidinger-Pauli, J. M., Guacci, V., Unal, E. and Koshland, D. E. (2008). Sister chromatid cohesion: a simple concept with a complex reality. *Annu. Rev. Cell Dev. Biol.* **24**, 105-129.
Pandey, R., Heidmann, S. and Lehner, C. F. (2005). Epithelial re-organization and dynamics of progression through mitosis in Drosophila separase complex mutants. *J. Cell Sci.* **118**, 733-742.
Papi, M., Berdougo, E., Randall, C. L., Ganguly, S. and Jallepalli, P. V. (2005). Multiple roles for separase auto-cleavage during the G2/M transition. *Nat. Cell Biol.* **7**, 1029-1035.
Queralt, E. and Uhlmann, F. (2005). More than a separase. *Nat. Cell Biol.* **7**, 930-932.
Rahman, A., Bannigan, A., Sulaman, W., Pechter, P., Blancaflor, E. B. and Baskin, T. I. (2007). Auxin, actin and growth of the *Arabidopsis thaliana* primary root. *Plant J.* **50**, 514-528.
Ramirez-Parra, E., López-Matas, M. A., Fründt, C. and Gutierrez, C. (2004). Role of an atypical E2F transcription factor in the control of Arabidopsis cell growth and differentiation. *Plant Cell* **16**, 2350-2363.
Sabatini, S., Beis, D., Wolkenfelt, H., Murfett, J., Guilfoyle, T., Malamy, J., Benfey, P., Leyser, O., Bechtold, N., Weisbeek, P. and Scheres, B. (1999). An auxin-dependent distal organizer of pattern and polarity in the Arabidopsis root. *Cell* **99**, 463-472.
Sak, A., Fegers, I., Groneberg, M. and Stuschke, M. (2008). Effect of separase depletion on ionizing radiation-induced cell cycle checkpoints and survival in human lung cancer cell lines. *Cell Prolif.* **41**, 660-670.
Serralbo, O., Pérez-Pérez, J. M., Heidstra, R. and Scheres, B. (2006). Non-cell-autonomous rescue of anaphase-promoting complex function revealed by mosaic analysis of *HOBBIT*, an arabidopsis *CDC27* homolog. *Proc. Natl. Acad. Sci. USA* **103**, 13250-13255.
Shepard, J. L., Amatruda, J. F., Finkelstein, D., Ziai, J., Finley, K. R., Stern, H. M., Chiang, K., Hersey, C., Barut, B., Freeman, J. L. et al. (2007). A mutation in separase causes genome instability and increased susceptibility to epithelial cancer. *Genes Dev.* **21**, 55-59.
Siomos, M. F., Badrinath, A., Pasierbek, P., Livingstone, D., White, J., Glotzer, M. and Nasmyth, K. (2001). Separase is required for chromosome segregation during meiosis I in *Caenorhabditis elegans*. *Curr. Biol.* **11**, 1825-1835.
Stegmeier, F., Visintin, R. and Amon, A. (2002). Separase, polo kinase, the kinetochore protein Slk19, and Spo12 function in a network that controls Cdc14 localization during early anaphase. *Cell* **108**, 207-220.
Sullivan, M. and Uhlmann, F. (2003). A non-proteolytic function of separase links the onset of anaphase to mitotic exit. *Nat. Cell Biol.* **5**, 249-254.
Suzuki, T., Nakajima, S., Inagaki, S., Hirano-Nakakita, M., Matsuoka, K., Demura, T., Fukuda, H., Morikami, A. and Nakamura, K. (2005). *TONSOKU* is expressed in S phase of the cell cycle and its defect delays cell cycle progression in arabidopsis. *Plant Cell Physiol.* **46**, 736-742.
Terret, M. E. and Jallepalli, P. V. (2006). Meiosis: separase strikes twice. *Nat. Cell Biol.* **8**, 910-911.
Tinker-Kulberg, R. L. and Morgan, D. O. (1999). Pds1 and Esp1 control both anaphase and mitotic exit in normal cells and after DNA damage. *Genes Dev.* **13**, 1936-1949.
Weingartner, M., Criqui, M. C., Meszaros, T., Binarova, P., Schmit, A. C., Helfer, A., Derevier, A., Erhardt, M., Bogre, L. and Genschik, P. (2004). Expression of a nondegradable cyclin B1 affects plant development and leads to endomitosis by inhibiting the formation of a phragmoplast. *Plant Cell* **16**, 643-657.
Wiedemeier, A. M., Judy-March, J. E., Hocart, C. H., Wasteneys, G. O., Williamson, R. E. and Baskin, T. I. (2002). Mutant alleles of arabidopsis *RADIALLY SWOLLEN 4* and *7* reduce growth anisotropy without altering the transverse orientation of cortical microtubules or cellulose microfibrils. *Development* **129**, 4821-4830.
Wirth, K. G., Wutz, G., Kudo, N. R., Desdouets, C., Zetterberg, A., Taghybeeglu, S., Seznec, J., Ducos, G. M., Ricci, R., Firnberg, N. et al. (2006). Separase: a universal trigger for sister chromatid disjunction but not chromosome cycle progression. *J. Cell Biol.* **172**, 847-860.
Yang, X., Boateng, K. A., Strittmatter, L., Burgess, R. and Makaroff. C. A. (2009). Arabidopsis separase functions beyond the removal of sister chromatid cohesion during meiosis. *Plant Physiol.* **151**, 323-333.
Zhu, Y., Dong, A., Meyer, D., Pichon, O., Renou, J. P., Cao, K. and Shen, W. H. (2006). Arabidopsis *NRP1* and *NRP2* encode histone chaperones and are required for maintaining postembryonic root growth. *Plant Cell* **18**, 2879-2892.